

# Drag force on a sphere in steady motion through a yield-stress fluid

Hervé Tabuteau

*Department of Physics and Astronomy, University of Western Ontario, London, Ontario, Canada N6A 3K7*

Philippe Coussot

*Department of Physics and Astronomy, University of Western Ontario, London, Ontario, Canada N6A 3K7  
and Institut Navier, Paris, France*

John R. de Bruyn<sup>a)</sup>

*Department of Physics and Astronomy, University of Western Ontario, London, Ontario, Canada N6A 3K7*

(Received 11 May 2006; final revision received 2 November 2006)

## Synopsis

We have studied the motion of spheres falling through yield-stress Carbopol gels. We measured the velocity of the falling sphere as a function of time and sphere density. Reproducible results were obtained when the experimental fluids were carefully prepared and homogenized. Three regimes of motion were observed. Spheres of high enough density reached a constant terminal velocity, as in Newtonian fluids. Below a critical density, the sphere came to a complete stop, while in an intermediate regime, the sphere continued to move but with a velocity which steadily decreased with time. We have also carefully characterized the rheological behavior of the fluids. The flow regimes observed for the falling sphere are analogous to those observed in creep tests for different applied stress levels. The yielding criterion and the drag force on the sphere obtained from our data are in excellent agreement with the longstanding but previously unconfirmed theoretical predictions of Beris *et al.* [J. Fluid Mech. **158**, 219–244 (1985)] and Beaulne and Mitsoulis [J. Non-Newtonian Fluid Mech. **72**, 55–71 (1997)]. © 2007 The Society of Rheology. [DOI: 10.1122/1.2401614]

## I. INTRODUCTION

Yield-stress fluids such as cement pastes, mineral slurries, drilling fluids, and natural muds are typically suspensions of coarse particles in a liquid. These particles can settle over time, since their density is larger than that of the suspending fluid. In many practical applications it is critical to control this settling to avoid the development of heterogeneities (as in food products) or to facilitate the transport of the suspended particles (as in

---

<sup>a)</sup>Author to whom correspondence should be addressed; electronic mail: [debruynd@uwo.ca](mailto:debruynd@uwo.ca)

drilling muds). The presence of a yield stress implies that settling of an object is only possible if the net gravitational force on the object exceeds the upward force due to the yield stress of the material. This principle has been the basis of practical rheometric tests for determining yield stress [Uhlherr *et al.* (2002), Schatzmann *et al.* (2003), Coussot (2005)].

Despite the apparent simplicity of the problem, the motion of an object through a yield-stress fluid remains poorly understood. It has long been observed that steady motion of the object required that a critical force be overcome. This is obviously a result of the material's yield stress, but the exact value of this critical force and the way in which the drag force increases with velocity once the object is moving have not been thoroughly investigated. Data in the literature are scarce and often poorly reproducible at low velocities [see the review of Chhabra and Uhlherr (1988)]. The most extensive studies are those of Atapattu *et al.* (1995) and, more recently, Merkak *et al.* (2006). Atapattu *et al.* (1995) carried out experiments in which spheres of different sizes were dropped under gravity into Carbopol gels with a range of properties. Jossic and Magnin (2001) and Merkak *et al.* (2006) studied the evolution of the velocity of spheres in response to an applied force. In particular, they observed that the roughness of the sphere's surface had a significant effect: the drag force was about 25% higher for rough spheres than for smooth spheres. The velocity dependence of the drag force on a sphere moving through foam [de Bruyn (2004), de Bruyn (2006)] and through Bentonite clay suspensions [Chafe and de Bruyn (2005)] has also been studied recently.

Much of the previous experimental work on yield-stress fluids has been done using Carbopol, a family of commercial polymers which form transparent gels when dispersed in water at concentrations on the order of tenths of a percent by weight. Carbopol gels are relatively simple yield-stress fluids. They exhibit no significant thixotropy or aging in their bulk properties, and their transparency makes them ideal for visualization experiments [Magnin and Piau (1990)]. Nonetheless, some previous work has found that the terminal velocity of a sphere falling through Carbopol could depend on the history of the sample — in particular, on the number of spheres that had previously been dropped into the same fluid [Hariharaputhiran *et al.* (1998), Horsley *et al.* (2004)]. This effect appears to suggest thixotropic behavior, but systematic studies of the motion of objects through fluids known to be thixotropic show a dependence of the velocity (or of the drag force) on the waiting time between the preparation of the sample and the measurement, or on the duration of the flow [Briscoe *et al.* (1992), Ferroir *et al.* (2004), Chafe and de Bruyn (2005)] that is not observed in Carbopol.

From a theoretical point of view, after various early attempts to provide approximate analytical expressions [du Plessis and Ansley (1967), Ansley and Smith (1967)], the yielding criterion (i.e., the force required to overcome the yield stress at the point of incipient motion) was determined analytically and numerically by Beris *et al.* (1985) by solving the equations for a regularized Bingham model. Blackery and Mitsoulis (1997) confirmed these results with numerical simulations using Papanastasiou's (1987) model for a Bingham fluid. The same group subsequently determined an expression for the force as a function of the velocity [Beaulne and Mitsoulis (1997)]. Using other regularization methods, Liu *et al.* (2002) confirmed these results for Bingham fluids.

The experimental validation of these theoretical developments nevertheless remains problematic: the only detailed comparison with an extensive set of data [the data of Atapattu *et al.* (1995)] indicates some discrepancy between theory and experiments. A quantitative validation of the theory requires not only a precise determination of the force-velocity curve over a wide range of velocities, but also a precise characterization of the rheological behavior of the fluid. The issue is complicated by the fact that the exis-

tence of a “true” yield stress is still under discussion in some quarters [Barnes and Walters (1985), Barnes (1999)]. In this paper we study the drag force on a spherical object moving in a yield-stress fluid through systematic experiments over a wide range of parameters coupled with a careful rheological analysis. We measured the variation of velocity with time for spheres falling through Carbopol gels, using spheres with a range of densities. At the lowest densities no motion was observed in steady state. We were able to discriminate between steady motion (a constant terminal velocity) and motion involving a progressive slowing of the sphere over long times, and to determine the yielding criterion accurately. We obtained reproducible results with our Carbopol samples simply by mixing them for a sufficiently long time prior to the experiment.

In Sec. II we describe the materials used and our experimental procedure. Our experimental results are presented in Sec. III and discussed in Sec. IV. Section V is a brief conclusion.

## II. EXPERIMENT

As experimental fluids we used two aqueous solutions of Carbopol ETD 2050 (No-veon), with concentrations  $\phi=0.5\%$  and  $2\%$  by weight. Carbopol is a commercial product based on cross-linked linear polyacrylic acid chains which is commonly used as a thickener. Carbopol powder was added slowly and with continuous stirring to de-ionized water. Sodium hydroxide solution was then added to raise the  $pH$  to 6. The suspension was then further mixed for ten days with a motorized mixer at 300 rpm to remove bubbles and completely homogenize the material. In bulk quantities these suspensions behave as yield-stress fluids due to the existence of a continuous network of interacting micron-sized hydrogel particles [Carnali and Naser (1992)]. The density  $\rho$  of both suspensions was measured to be  $1000 \text{ kg/m}^3$  to within  $0.5\%$  at a temperature of  $22^\circ\text{C}$ .

Rheometric measurements were carried out under controlled strain using an ARES RHS rheometer equipped either with stainless steel concentric cylinders (inner radius  $r_1=16 \text{ mm}$ , outer radius  $r_2=17 \text{ mm}$ , immersed length  $34 \text{ mm}$ ) or with parallel plates of diameter  $50 \text{ mm}$  and separation  $1.5 \text{ mm}$ . Sandpaper with a roughness on the order of  $200 \mu\text{m}$  was glued onto the parallel plates to prevent wall slip. A temperature-controlled circulating fluid bath was used to maintain the tool at a temperature of  $22^\circ\text{C}$ . The flow curve was measured by imposing a steady shear and recording the corresponding steady-state stress; measurements were done starting at high shear rate and working downwards. The linear viscous and elastic moduli were measured by applying a small-amplitude oscillatory shear. Measurements were also performed using a TA Instruments AR 1000 controlled-stress rheometer equipped with parallel plates of diameter  $40 \text{ mm}$  with a gap of  $1.5 \text{ mm}$ . As above, the plates were covered with sandpaper to prevent wall slip. In this case, a constant stress was applied and the resulting deformation measured as a function of time. The material was presheared at  $300 \text{ s}^{-1}$  and left at rest for  $30 \text{ s}$  before each measurement at constant stress.

The motion of spheres moving through suspensions of Carbopol was studied using a high-speed video camera (MotionScope, Red Lake Imaging) with frame rates typically in the range of  $60\text{--}250 \text{ frames/s}$ . The position of the bottom edge of the sphere in each frame was measured with a digital cross hair and converted from pixel units to true distance. We used a series of  $1.27\text{-cm}$ -diam metal spheres of different densities  $\rho_s$ . All of these objects had a surface roughness well below  $1 \mu\text{m}$  (the roughness of one steel ball was measured with a profilometer to be  $\pm 0.1 \mu\text{m}$  over  $1 \text{ mm}$ ), with the exception of one which was machined to give a roughness measured to be  $\pm 4 \mu\text{m}$  over  $1 \text{ mm}$ . We also used a hollow plastic ping-pong ball of diameter  $3.96 \text{ cm}$  with a hole cut into its top. The

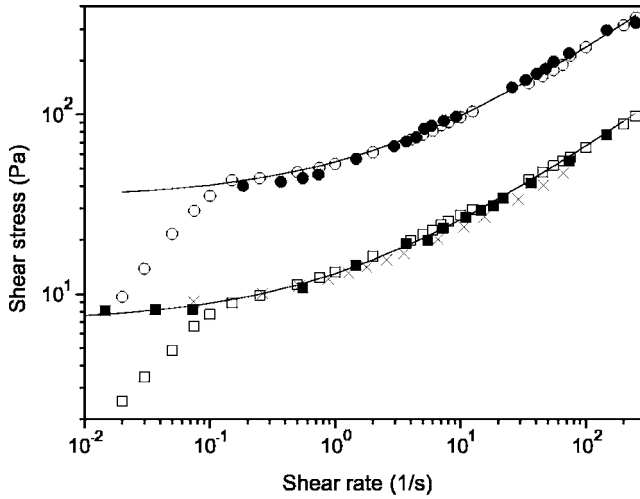


FIG. 1. The steady-state shear stress  $\tau$  plotted as a function of shear rate  $\dot{\gamma}$  for the two concentrations of Carbopol studied (squares:  $\phi=0.5$ , circles:  $\phi=2.0$ ). Data indicated by solid symbols were measured with the parallel plate geometry, and by open symbols disks with the Couette geometry, both with the controlled strain rheometer. The data plotted as crosses were measured in controlled stress tests.

density of the ping-pong ball was varied by gluing a number of small steel beads inside it before each run, after which the hole was covered with a small piece of duct tape. Apart from the tape, which was at the top of the ball as it moved through the material, the surface roughness of the ping-pong ball was estimated to be on the order of  $10 \mu\text{m}$ .

Except where explicitly noted below, the balls were dropped into Carbopol suspensions contained in a Plexiglas vessel having a square cross section with length and width  $L=25 \text{ cm}$ ,  $25 \text{ cm}$  deep. After the container was filled with the fluid, the sphere was positioned a known distance ( $5 \text{ cm}$ , except as noted below) above the free surface on an adjustable diaphragm. The diaphragm was opened to release the sphere and its motion recorded with the high-speed camera. The maximum duration of the video, which was limited by the camera's memory, was  $10 \text{ s}$ , so for slow runs we recorded several videos at different times during the fall. In some cases we released the sphere from below the free surface by hand. All experiments were carried out at room temperature, which was  $22 \text{ }^\circ\text{C}$ .

### III. RESULTS

#### A. Rheometry

Figure 1 shows the flow curves for the two concentrations of Carbopol. Data from both stress and strain controlled measurements are shown, in the latter case for both Couette and parallel plate geometries.

For the Couette geometry, the shear stress at the inner cylinder is plotted as a function of the apparent shear rate,  $\dot{\gamma}=\Omega r_1/(r_2-r_1)$ . Here  $\Omega$  is the angular velocity of the inner cylinder. The shear rate within a yield-stress fluid can be inhomogeneous, but since the gap-to-diameter ratio  $(r_2-r_1)/r_1$  is small, this effect is expected to be small except at very low velocities and will be neglected.

For the parallel plate geometry, the shear rate and shear stress vary with radial position within the gap. This can be accounted for using the classical formula [Coleman *et al.* (1966)]

$$\tau_R = \frac{M}{2\pi R^3} \left( 3 + \frac{\dot{\gamma}_R}{M} \frac{\partial M}{\partial \dot{\gamma}_R} \right) \quad (1)$$

in which  $\tau_R$  and  $\dot{\gamma}_R = \Omega R/h$  are the shear stress and shear rate at radial position  $R$ , respectively, where  $R$  is the radius of the circular plates,  $h$  the gap between them, and  $M$  the torque. From Eq. (1) we can get  $\tau_R$  as a function of  $\dot{\gamma}_R$ , the constitutive equation for the material in simple shear. The software that controls the rheometer, however, calculates an apparent shear stress  $\tau_{app} = 3M/2\pi R^3$  and provides  $\tau_{app}$  as a function of  $\dot{\gamma}_R$ . From our data we find that  $\tau_{app}$  is well described by a Herschel-Bulkley model of the form  $\tau_{app} = \tau_c + K^* \dot{\gamma}_R^n$ , where  $\tau_c$ ,  $K^*$ , and  $n$  are fitting parameters. Given this we can deduce from Eq. (1) that the constitutive equation of the fluid in simple shear should have a similar form with the coefficient  $K^*$  replaced by  $K = (1+n/3)K^*$ :

$$\tau_R = \tau_c + K \dot{\gamma}_R^n. \quad (2)$$

Since we can rewrite the equation for  $\tau_{app}$  as  $\tau_{app} = \tau_c + K((K^*/K)^{1/n} \dot{\gamma}_R)^n$ , we see that  $\tau_R(\dot{\gamma}_R) = \tau_{app}((K^*/K)^{1/n} \dot{\gamma}_R)$ . The parallel-plate data shown in Fig. 1 have been corrected in this way.

The Couette and parallel-plate data agree well except at shear rates below  $0.1 \text{ s}^{-1}$ , where the Couette data fall below the parallel-plate data. This is likely due to wall slip at the smooth tool surfaces in the Couette geometry. The data for the higher concentrations at these low shear rates were noisy, possibly due to shear banding, and are not shown in the figure. Neglecting this region,  $\tau_R$  is well described by a Herschel-Bulkley model in the form of Eq. (2) with  $n=0.5$ . For  $\phi=0.5\%$  we find  $\tau_c=7 \text{ Pa}$  and  $K=6 \text{ Pa s}^{0.5}$ , while for  $\phi=2\%$ ,  $\tau_c=34 \text{ Pa}$  and  $K=20.4 \text{ Pa s}^{0.5}$ . Measurements of the linear viscous and elastic moduli under small-amplitude oscillatory shear show that the elastic modulus is at least ten times larger than the viscous modulus for frequencies between 0.1 and 10 Hz.

The Herschel-Bulkley model implicitly assumes that the material is in a solid regime—that is, that  $\dot{\gamma}=0$  and the material does not flow—for  $\tau < \tau_c$ , and in a liquid regime for larger stresses. Creep measurements made with the controlled stress rheometer for  $\phi=0.5\%$ , shown in Fig. 2, provide further insight into the material behavior. These data display distinct solid and liquid regimes: below a certain stress value  $\tau_0$  the deformation of the material reaches a constant value and remains constant even over very long times, but for an applied stress above a higher value  $\tau_c$  the material reaches a steady state in which it flows with a constant shear rate  $\dot{\gamma}$ . For stresses intermediate between  $\tau_0$  and  $\tau_c$ , the deformation  $\gamma(t)$  at first increases then tends to plateau. Over longer times  $\gamma(t)$  increases further, but with a logarithmic slope of the deformation vs. time curve that is much less than 1. This gives a deformation proportional to  $t^b$ , with  $b < 1$ , so the shear rate  $\dot{\gamma} \sim t^{b-1}$ . This shear rate decreases in time, never reaching a steady state, implying that in this intermediate regime there are no stable flows over long times. In physical terms, this likely corresponds to the fact that at these values of  $\tau$ , the initial structure of the material is not broken but rather undergoes a finite deformation even after long times, possibly accompanied by some local structural rearrangement. Here we consider this ultimate saturation of the deformation to indicate that the material is still in the solid regime under these conditions. The value of  $\tau_c$  at which the material enters the liquid regime—slightly less than 8 Pa—corresponds well with that found from the controlled rate measurements of Fig. 1.

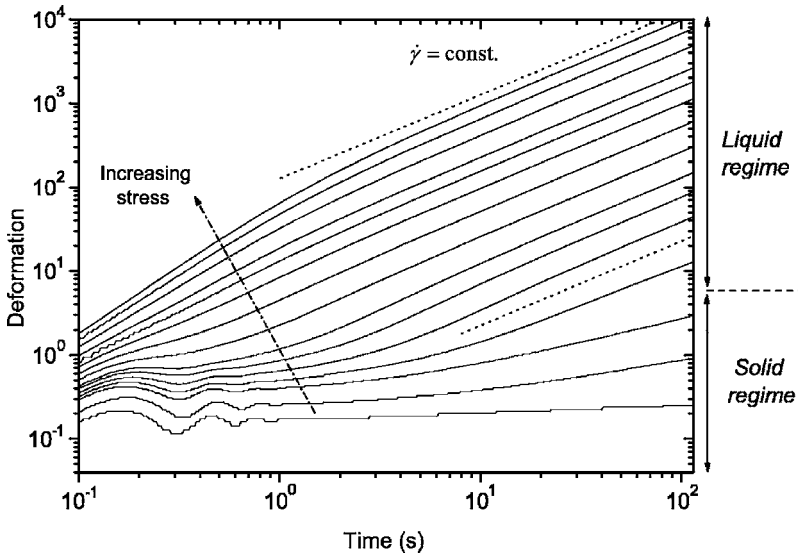


**FIG. 2.** The deformation  $\gamma$  of a 0.5% Carbopol suspension as a function of time for different applied stress levels, measured with a parallel-plate geometry using the controlled stress rheometer. Here  $\gamma = \alpha R/h$ , where  $\alpha$  is the rotation angle of the moving plate. From bottom to top, the lines correspond to stresses of 4, 5.4, 8.1, 9.1, 10.1, 11.1, 12.1, 14.1, 16.8, 20.2, 23.6, 26.9, 33.7, 40.4, and 40.7 Pa. The dotted lines have logarithmic slope 1, corresponding to a constant shear rate.

**B. Falling spheres**

Figure 3 shows the results of falling sphere experiments performed with the variable-density ping-pong ball. The figure shows the penetration depth as a function of time with logarithmic scales. The same data are plotted with linear scales in Fig. 4. At early times some oscillations in the depth appear [Akers and Belmonte (2006), Jayaraman and Bel-

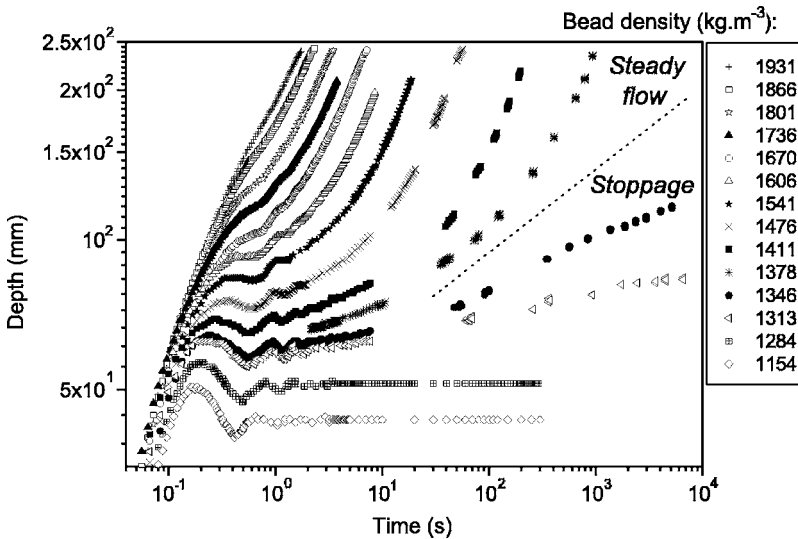


**FIG. 3.** The depth as a function of time for the variable-density ping-pong ball falling through a 0.5% Carbopol suspension. The different symbols correspond to different densities as indicated.

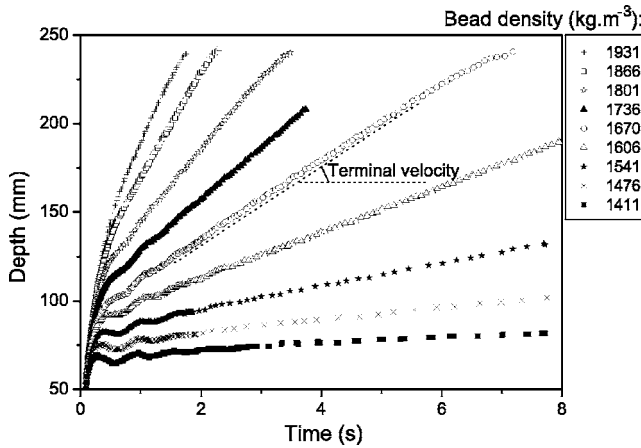


FIG. 4. The higher-density data from Fig. 3 plotted with linear axes. The terminal velocity is the slope of the linear portion of the curve at long times.

monte (2003)]. These result from the interaction between the inertia of the sphere and the elastic behavior of the material in its solid regime and will be discussed elsewhere. After the end of these oscillations we can again distinguish three regimes: for densities above a critical density  $\rho_c$  the depth of the sphere increases linearly with time, corresponding to steady-state motion at a density-dependent terminal velocity  $V$ . For a density smaller than a lower value  $\rho_0$ , the sphere rapidly comes to rest after the initial transient. For intermediate densities it never reaches a steady state, and its velocity steadily decreases with time at long times, as indicated by a logarithmic slope in Fig. 3 that is significantly less than one. The decrease in velocity visible in Fig. 4 for depths larger than about 230 mm occurs as the sphere approaches the bottom of the sample vessel, suggesting that the bottom does not affect the sphere's motion before it reaches this depth.

There is a strong similarity between the behavior of the falling spheres and the results of the creep tests shown in Fig. 2. In analogy with the above discussion, we interpret these data as follows. For densities higher than  $\rho_c$ , the sphere reaches a steady velocity and is surrounded by a volume of material which can be considered to be in the fluid regime. For densities below  $\rho_0$ , the sphere remains motionless and the material around it is in the solid regime. For intermediate densities the sphere moves with a continuously decreasing speed, possibly due to localized changes in the material structure close to the interface with the sphere. In this regime the suspension surrounding the sphere cannot be considered to be totally fluidized. We take the material surrounding the sphere to be liquid for  $\rho > \rho_c$ , and associate this density with the critical stress  $\tau_c$  found in the rheometric measurements.

We note that the terminal velocity was independent of the number of spheres dropped through the fluid—our results were quite reproducible, in contrast to what was found in earlier work [Hariharaputhiran *et al.* (1998), Horsley *et al.* (2004)]. We attribute the reproducibility of our results to careful preparation of the suspensions, and more precisely to the long mixing times used. Indeed, when we prepared material using significantly shorter mixing times (on the order of only one day), the data were much less reproducible.

The terminal velocity was also independent of the depth of the vessel for sufficiently deep vessels: no significant difference in  $V$  was found between experiments using vessels of depths 25 and 60 cm. The influence of the container walls was investigated by mea-

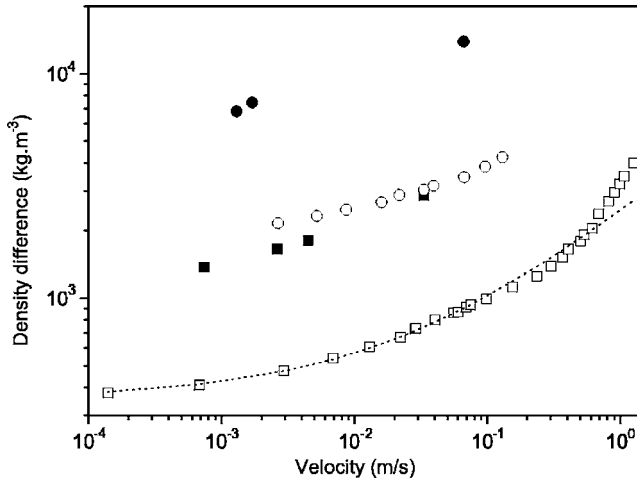


**FIG. 5.** The density difference  $\Delta\rho$  of the spheres falling through Carbopol suspensions plotted against the terminal velocity. Open symbols:  $d=3.96$  cm; solid symbols,  $d=1.27$  cm. The squares are for a Carbopol concentration of 0.5% and the circles for  $\phi=2\%$ . The dotted line is the prediction of a theoretical model for the large spheres in the more dilute material, as discussed in the text.

asuring the terminal velocity for different values of the ratio  $L/d$ , where  $L$  is the width of the container and  $d$  the diameter of the sphere, for the same density difference. In agreement with the results of Atapattu *et al.* (1990), we found the velocity to be constant for  $L/d \geq 10$ , and to decrease with decreasing  $L/d$  below this value. This effect is most important for the largest spheres used, for which this ratio is 6.3. In this case the terminal velocity is only about 10% smaller than the asymptotic value for large aspect ratio. In what follows we will neglect this effect. The height from which the sphere was released affected the motion in the initial transient regime, but we observed no significant difference in the terminal velocity for different release heights. The same terminal velocity was also obtained when the sphere was released below the fluid surface. Finally, we found no significant effect of surface roughness on the terminal velocity, for roughnesses ranging from 0.1 to several  $\mu\text{m}$ . Since this range of roughness goes from smaller than the typical length scale of the microscopic structure of the Carbopol to larger than that length scale, this suggests that wall slip is unimportant and that roughness plays a negligible role in our experiments. This may also be a consequence of the good homogenization of the material.

#### IV. DISCUSSION

The drag force on an object moving through a Newtonian or a power-law fluid is proportional to some power of the velocity [Dazhi and Tanner (1985)]. For our spheres falling at constant speed through a yield-stress fluid, we expect the net downward force  $F_g = (1/6)\pi d^3 g \Delta\rho$ , where the density difference  $\Delta\rho = \rho_s - \rho$  to be balanced by an upward force that is the sum of a constant term related to the yield stress and a “viscous” term depending on the velocity. This hypothesis is confirmed by our data: In Fig. 5 we plot  $\Delta\rho$  against the terminal velocity  $V$  measured with a variety of falling spheres in the two Carbopol samples. The results for the ping-pong ball with different densities follow a curve similar in shape to the flow curve plotted in Fig. 1. The dotted line in Fig. 5 is a fit to an equation of the form  $\Delta\rho = \Delta\rho_c + K_0 V^n$  with the exponent  $n=0.5$ , and describes the

data reasonably well for velocities up to about 0.1 m/s. The drag force on an object moving through a foam has been shown to have a similar behavior [de Bruyn (2004)].

The general problem of the motion of a sphere through a yield-stress fluid is described by the complete set of equations of motion, along with a constitutive equation, which we take to be the Herschel-Bulkley equation, Eq. (2), and appropriate boundary conditions. While this problem is in general complex, it is readily shown that three dimensionless numbers parameterize the problem. They are the generalized Reynolds number

$$\text{Re} = \frac{\rho_0 V^2}{K(V/d)^n}, \quad (3)$$

the Bingham number

$$\text{Bi} = \frac{\tau_c}{K(V/d)^n}, \quad (4)$$

and the yield number

$$Y = \frac{3\tau_c}{gd\Delta\rho}. \quad (5)$$

In an attempt to generalize the simple relation between the drag coefficient  $C_D = 4gd\Delta\rho/3\rho_0V^2$  and the Reynolds number that holds for Newtonian fluids, Ansley and Smith (1967) proposed to express the drag coefficient for yield-stress fluids as

$$C_D = \frac{4 \text{Bi}}{Y \text{Re}} = 24X(n) \left( \frac{1 + k \text{Bi}}{\text{Re}} \right) = \frac{24X(n)}{Q}, \quad (6)$$

where the so-called dynamical parameter  $Q = \text{Re}/(1 + k \text{Bi})$ . The numerical coefficient  $k$  was postulated to be equal to 1 by Ansley and Smith (1967) and found from numerical simulations to be 0.823 [Beaulne and Mitsoulis (1997)]. Atapattu *et al.* (1995), on the other hand, fit their data to Eq. (6) and found  $k=0.614$ .  $X(n)$  is a drag-correction factor for power-law fluids which has been determined by Gu and Tanner (1985) to be 1.42 for  $n=0.5$ . In Fig. 6 we plot our data in the form of the drag coefficient  $C_D$  as a function of  $Q$ . The solid line corresponds to Eq. (6) with the numerically determined value of 0.823 for  $k$ . The agreement between our data and the theoretical predictions is excellent over seven decades in  $Q$ , with slight deviations from the predicted  $1/Q$  dependence becoming apparent only for  $Q > 10$ . This is in contrast with the data of Atapattu *et al.* (1995), for which some discrepancy with the theory was observed, even for small values of  $Q$ .

In fact Fig. 6 does not permit a particularly stringent comparison between the data and the predictions of Eq. (6), since any deviation visible on a log-log graph spanning eight decades must be rather large. A more sensitive plot is obtained by rewriting Eq. (6) in the form

$$\frac{1}{Y} = 6kX(n) + \frac{6X(n)}{\text{Bi}} = 7 + \frac{8.52}{\text{Bi}}, \quad (7)$$

where we have used the theoretical value of Beaulne and Mitsoulis (1997) for  $k$  and the above value of  $X(n)$  for  $n=0.5$ . This theoretical prediction, which we emphasize is based on numerical predictions and involves no free parameters, is compared with our data in Fig. 7. We find extremely good agreement for  $\text{Bi}^{-1} \lesssim 3$ . In addition, we find the critical value  $Y_c$  of the yield parameter above which there is no motion of the sphere (that is, the reciprocal of the intercept of Fig. 7 at  $\text{Bi}^{-1}=0$ ) to be 0.145, in excellent agreement with the value of 0.143 predicted by Beris *et al.* (1985) and Blackery and Mitsoulis (1997).

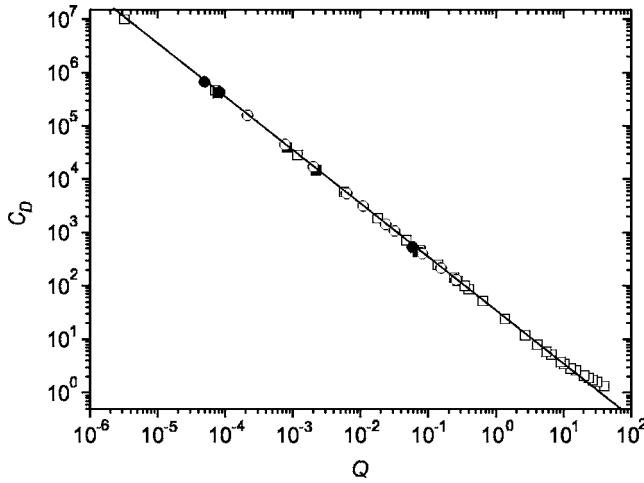


**FIG. 6.** The drag coefficient as a function of the dynamic parameter  $Q$  for the data of Fig. 5. The symbols have the same meaning as in that figure. The solid line is the prediction of Eq. (6) using the numerically calculated values of the coefficients.

This provides experimental confirmation of the critical conditions for the onset of steady motion of a sphere through a yield-stress fluid. We note that this good agreement depends on the correct identification of the dynamical regimes observed in both the rheometry and the falling sphere experiments described above.

For  $Bi^{-1} > 3$  the experimental data deviate from the theoretical curve; this deviation is even more clear when the data are plotted with linear axes as in the inset to Fig. 7. For simple power-law fluids,  $Y^{-1} = 6X(n)Bi^{-1}$ . Our data do not show this behavior when  $Bi$  is small, i.e., when the shear-dependent term in Eq. (2) becomes much larger than the constant term. This may be due to the increasing importance of inertial effects as  $V$  increases. To investigate this, we plot  $Y^{-1}$  as a function of the generalized Reynolds

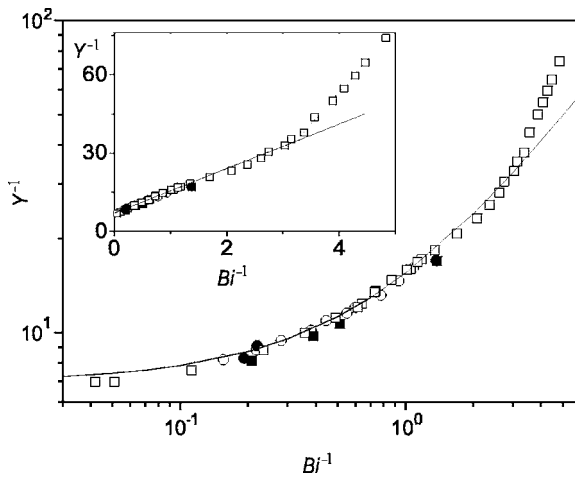


**FIG. 7.** The data of Fig. 6 plotted as  $Y^{-1}$ , the reciprocal of the yield number, as a function of  $Bi^{-1}$ , the reciprocal of the Bingham number. The inset shows the same data plotted with linear axes. In both cases the solid line corresponds to Eq. (7); the dotted line shows the deviation of data from the theory.

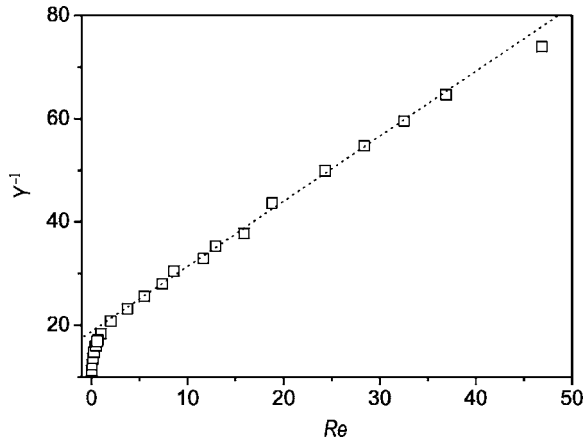


**FIG. 8.**  $Y^{-1}$  as a function of the generalized Reynolds number  $Re$ . The dotted line is drawn through the data for  $Re > 2$ .

number in Fig. 8. For large  $Y^{-1}$ , we find that  $Y^{-1}$  increases linearly with  $Re$ . This implies that the drag force is also linear in the Reynolds number (which here scales as  $V^{2-n}$ ), and suggests an analogy with the well-developed turbulent regime in Newtonian fluids. In that case the drag coefficient is approximately constant, leading to a drag force proportional to the Reynolds number (which in that case scales as  $V$ ). In the present case, however, the regime where the drag force is proportional to  $Re$  occurs just at the end of the laminar regime, where inertial effects are still small, whereas for Newtonian fluids there is a wide transitional regime. Further data covering a larger range of velocities and experimental parameters are required to confirm the generality of this finding.

## V. CONCLUSION

Careful preparation of the Carbopol suspensions used in our experiments made it possible for us to obtain reproducible results. Careful determination of the yielding condition in rheometrical experiments and from the motion of spheres falling through the suspensions led to very good agreement between our experimental data and previous theoretical predictions for the drag force on a sphere moving through a yield-stress fluid at large  $Bi$ . These results give confidence in the application of current theory to practical situations once the rheological behavior of the material has been carefully determined. Further studies of the regime in which inertia becomes important are required, but our preliminary results suggest that this regime might be very different from the analogous regime in Newtonian fluids.

## ACKNOWLEDGMENTS

This research was supported by the Natural Science and Engineering Research Council of Canada. P. Coussot gratefully acknowledges a visiting fellowship from the Center for Chemical Physics at The University of Western Ontario. We are grateful to M. Rogers and S. W. Morris for the use of the controlled-stress rheometer and to F. Opong and D. Sikorski for helpful discussions.

## References

- Akers, B., and A. Belmonte, "Impact dynamics of a solid sphere falling into a viscoelastic micellar fluid," *J. Non-Newtonian Fluid Mech.* **135**, 97–108 (2006).
- Ansley, R. W., and T. N. Smith, "Motion of spherical particles in a Bingham plastic," *AIChE J.* **13**, 1193–1196 (1967).
- Atapattu, D. D., R. P. Chhabra, and P. H. T. Uhlherr, "Creeping sphere motion in Herschel-Bulkley fluids: Flow field and drag," *J. Non-Newtonian Fluid Mech.* **59**, 245–265 (1995).
- Atapattu, D. D., R. P. Chhabra, and P. H. T. Uhlherr, "Wall effect for spheres falling at small Reynolds number in a viscoplastic medium," *J. Non-Newtonian Fluid Mech.* **38**, 31–42 (1990).
- Barnes, H. A., and K. Walters, "The yield stress myth?," *Rheol. Acta* **24**, 323–326 (1985).
- Barnes, H. A., "The yield stress - A review or 'παντα ρει' — everything flows?," *J. Non-Newtonian Fluid Mech.* **81**, 133–178 (1999).
- Beaulne, M., and E. Mitsoulis, "Creeping motion of a sphere in tubes filled with Herschel-Bulkley fluids," *J. Non-Newtonian Fluid Mech.* **72**, 55–71 (1997).
- Beris, A. N., J. A. Tsamopoulos, R. C. Armstrong, and R. A. Brown, "Creeping motion of a sphere through a Bingham plastic," *J. Fluid Mech.* **158**, 219–244 (1985).
- Blackery, J., and E. Mitsoulis, "Creeping motion of a sphere in tubes filled with a Bingham plastic material," *J. Non-Newtonian Fluid Mech.* **70**, 59–77 (1997).
- Briscoe, B. J., M. Glaese, P. F. Luckam, and S. Ren, "The falling of spheres through Bingham fluids," *Colloids Surf.* **65**, 69–75 (1992).
- Carnali, J. O., and M. S. Naser, "The use of dilute solution viscosimetry to characterize the network properties of carbopol microgels," *Colloid Polym. Sci.* **270**, 183–193 (1992).
- Chafe, N. P., and J. R. de Bruyn, "Drag and relaxation in a bentonite clay suspension," *J. Non-Newtonian Fluid Mech.* **131**, 44–52 (2005).
- Chhabra, R. P., and P. H. T. Uhlherr, "Static equilibrium and motion of spheres in viscoplastic liquids," in *Encyclopedia of Fluid Mechanics*, edited by N. P. Cheremisinoff (Gulf, Houston, 1988), Chap. 21, Vol. 7.
- Coleman, B. D., H. Markowitz, and W. Noll, *Viscometric Flows of Non-Newtonian Fluids* (Springer-Verlag, Berlin, 1966).
- Coussot, P., *Rheometry of Pastes, Suspensions and Granular Materials* (Wiley, New York, 2005).
- Dazhi, G., and R. I. Tanner, "The drag on a sphere in a power-law fluid," *J. Non-Newtonian Fluid Mech.* **17**, 1–12 (1985).
- de Bruyn, J. R., "Transient and steady-state drag in foam," *Rheol. Acta* **44**, 150–159 (2004).
- de Bruyn, J. R., "Age dependence of the drag force in an aqueous foam," *Rheol. Acta* **45**, 803–811 (2006).
- du Plessis, M. P., and R. W. Ansley, "Settling parameters in solids pipelining," *J. Pipeline Div.* **2**, 1–16 (1967).
- Ferroir, T., H. T. Huynh, X. Chateau, and P. Coussot, "Motion of a solid object through a thixotropic paste," *Phys. Fluids* **16**, 594–601 (2004).
- Gu, D., and R. I. Tanner, "The drag on a sphere in a power-law fluid," *J. Non-Newtonian Fluid Mech.* **17**, 1–12 (1985).
- Hariharaputhiran, M., R. S. Subramanian, G. A. Campbell, and R. P. Chhabra, "The settling of spheres in a viscoplastic fluid," *J. Non-Newtonian Fluid Mech.* **79**, 87–97 (1998).
- Horsley, M. R., R. R. Horsley, K. C. Wilson, and R. L. Jones, "Non-Newtonian effects on fall velocities of pairs of vertically aligned spheres," *J. Non-Newtonian Fluid Mech.* **124**, 147–152 (2004).
- Jayaraman, A., and A. Belmonte, "Oscillations of a solid sphere falling through a wormlike micellar fluid," *Phys. Rev. E* **67**, 065301, 1–4 (2003).
- Jossic, L., and A. Magnin, "Drag and stability of objects in a yield stress fluid," *AIChE J.* **47**, 2666–2672 (2001).
- Liu, B. T., S. J. Muller, and M. M. Denn, "Convergence of a regularization method for creeping flow of a Bingham material about a rigid sphere," *J. Non-Newtonian Fluid Mech.* **102**, 179–191 (2002).
- Magnin, A., and J.-M. Piau, "Cone-and-plate rheometry of yield stress fluids. Study of an aqueous gel," *J. Non-Newtonian Fluid Mech.* **36**, 85–108 (1990).
- Merkak, O., L. Jossic, and A. Magnin, "Spheres and interactions between spheres moving at very low velocities

- in a yield stress fluid," *J. Non-Newtonian Fluid Mech.* **133**, 99–108 (2006).
- Papanastasiou, T. C., "Flow of materials with yield," *J. Rheol.* **31**, 385–404 (1987).
- Schatzmann, M., P. Fischer, and G. R. Bezzola, "Rheological behavior of fine and large particle suspensions," *J. Hydraul. Eng.* **129**, 796–803 (2003).
- Uhlherr, P. H. T., J. Guo, T. N. Fang, and C. Tiu, "Static measurement of yield stress using a cylindrical penetrometer," *Korea-Aust. Rheol. J.* **14**, 17–23 (2002).